Available online at www.sciencedirect.com
ScienceDirect
Journal of the European Ceramic Society 28 (2008) 1527–1534
www.elsevier.com/locate/jeurceramsoc

Sintering and grain growth in SiO_2 doped Nd:YAG

Sujarinee Kochawattana[a,1], Adam Stevenson[a], Sang-Ho Lee[a], Mariola Ramirez[a], Venkatraman Gopalan[a], John Dumm[b], Vida K. Castillo[c], Gregory J. Quarles[c], Gary L. Messing[a,*]

[a] *Department of Materials Science and Engineering and the Materials Research Institute, The Pennsylvania State University, University Park, PA 16802, USA*
[b] *Advanced Materials Development Center, II-VI Inc., Saxonburg, PA 16056, USA*
[c] *VLOC, subsidiary of II-VI Inc., 7826 Photonics Drive, New Port Richey, FL 34655, USA*

Available online 18 January 2008

Abstract

Densification and grain growth in pure YAG, SiO_2 doped YAG and SiO_2 doped Nd:YAG were explored. The activation energy for densification (235 kJ/mol) in pure YAG is lower than that of grain growth (946 kJ/mol) which is unusual in ceramic systems. Consequently, pure YAG sinters to near full density (>99.9%) at 1700 °C with little grain growth (1.2 μm average grain size). The remaining large pores (radius > 2 μm) were determined to be thermodynamically stable because their coordination number with grains was >6. The stability of these pores underscores the importance of powder processing and forming in fabricating transparent YAG. SiO_2 doped YAG sinters to near full density 100 °C lower than pure YAG because SiO_2 enables liquid phase sintering and the removal of large pores. The addition of Nd_2O_3 further enhances both densification and grain growth at temperatures below 1700 °C. Above 1700 °C higher concentrations of Nd^{3+} suppressed grain growth, possibly due to solute drag.

Keywords: YAG; Sintering; Powder-solid state reaction; Grain growth; Optical properties

1. Introduction

The need for materials that combine transparency, high strength, scratch resistance, and thermal stability has driven the development of transparent ceramics for armor, optical, and laser applications. Coble of General Electric (GE) reported "transparent" ceramics in a patent wherein MgO doped Al_2O_3 was sintered to full density and had an in-line transmission of 40–50% between 400 and 600 nm.[1] Coble's patent was the first to demonstrate that polycrystalline ceramics, even those exhibiting birefringence, can have substantial light transmission at optical wavelengths by eliminating all porosity during sintering. However, it is known that the optical transmission of non-cubic, birefringent polycrystalline ceramics is limited by scattering at grain boundaries and is the primary cause of their translucency when the ceramic is fully dense. Thus, the quest for truly transparent polycrystalline materials has focused attention on sintering cubic crystal structure ceramics (e.g. MgO, $MgAl_2O_4$).

In 1970, Anderson of GE patented a process for sintering 90% Y_2O_3–10% ThO_2 that had >70% in-line transmission at optical wavelengths.[2] This material, called Yttralox, was proposed for use in lamp envelopes, high temperature windows, and high temperature lenses, but commercialization was limited because these ceramics required sintering temperatures of 2000–2200 °C.[2] This material represented a significant technological advance because a sintered polycrystalline material had >70% transmission. Benecke et al. reported hot pressing MgO between 775 and 975 °C and annealing to transparency at 1300 °C, and successfully demonstrated that transparent ceramics could be produced at substantially lower temperatures than Yttralox.[3] After 1970 many patents were issued for sintering and hot pressing $MgAl_2O_4$, MgO, and Y_2O_3 to 70–80% in-line transmission, and interest in each of these and other materials (e.g. ALON, PLZT, BeO, Al_2O_3, ZnS, ZnSe) resulted in successful commercial products such as lamp envelopes, windows, domes, and lenses.[4–7]

Apetz and van Bruggen showed that porosity has a dramatic impact on light transmission because of the refractive index

* Corresponding author. Tel.: +1 814 865 2262; fax: +1 814 865 2917.
E-mail address: Messing@ems.psu.edu (G.L. Messing).
[1] Current address: Chulalongkorn University, Bangkok, Thailand.

0955-2219/$ – see front matter © 2007 Elsevier Ltd. All rights reserved.
doi:10.1016/j.jeurceramsoc.2007.12.006

difference between pores and the surrounding ceramic matrix ($\Delta n \approx 0.76$ for alumina).[8] Their work showed that even nanopores (those with radii below 100 nm) at a concentration below 0.01 vol% result in substantial scattering and thus underscored the importance of density for achieving transparency.

Recently, Krell et al. produced fully dense, polycrystalline Al_2O_3 with an in-line transmission >70% at 645 nm by reducing the average grain size to 600 nm, which was similar to the optical wavelengths (380–750 nm).[9] At that grain size, Apetz and van Bruggen showed that geometric optics break down and only Raleigh–Ganz–Debye scattering occurs at grain boundaries, mitigating the effects of birefringence.[8] For the first time, a nearly transparent polycrystalline ceramic with non-cubic crystal structure was produced.

The literature reports hundreds of papers concerned with the processing and sintering of "transparent" ceramics. Unfortunately, many of these ceramics are not truly transparent because they contain a certain fraction of porosity, second phases, or they are birefringent. Although many of these materials are "transparent" to the eye, measures of light transmission, if reported, show the materials to have <50% in-line transmission at optical wavelengths. We propose that the term *transparent* be reserved for ceramics with at least 95% of the theoretical transmission over the wavelengths of interest. For example, the theoretical transmission of YAG is 84% at 1064 nm. Thus, the transmission must be >79.8% to be described as "transparent". Thus, YAG ceramics with an in-line transmission <79.8% should be classified as translucent to distinguish them from the exceptional case of a truly transparent ceramic.

2. Polycrystalline laser materials

Greskovich and Chernoch reported the first laser gain in a polycrystalline oxide ceramic.[10] The optical absorption spectra and fluorescence lifetimes of 1% Nd_2O_3–89% Y_2O_3–10% ThO_2 (or Nd^{3+} doped Yttralox) sintered to full density were similar to state of the art Nd:YAG single crystals and Nd:glass laser gain media. The slope efficiency of their ceramics was 0.098% while Nd:glass tested in the same configuration had a slope efficiency of 0.44%. Their report was an important proof of concept; sufficiently well processed polycrystalline materials could exhibit laser gain, but these materials were not commercialized due to their low efficiency.

de With and van Dijk reported the sintering of $Y_3Al_5O_{12}$ (yttrium aluminum garnet, or YAG) to translucency starting with either mixed oxides (solid state reaction) or co-precipitated powders as long as sintering aids (SiO_2 and MgO) were used.[11] Ikesue et al. reported using SiO_2 to sinter 0.9 at% Nd:YAG ceramics to sufficient transparency to achieve a laser slope efficiency similar to Czochralski grown single crystals[12]. Concurrent with the report of Ikesue et al., Yagi et al. of Konoshima Chemical Inc. and colleagues at the Institute for Laser Science, University for Electro-communication (Tokyo, Japan) developed high quality YAG laser materials.[12,13] Recently, there have been many reports of sintering YAG based systems and several sesquioxide materials (e.g. Y_2O_3, Sc_2O_3) to transparency.[14–17] Table 1 lists some of the other ceramics used for optical applications and their respective theoretical transmissions, which depend on their refractive indices, at 1064 nm.

The solid state reaction (SSR) and chemical co-precipitation processes are the most important methods for synthesizing YAG. Ikesue et al.'s work demonstrates the SSR approach; a process in which Al_2O_3 and Y_2O_3 powders are mixed in stoichiometric amounts and phase formation occurs during sintering, but before the compact densifies. The benefit of the SSR process is that commercially available powders can be used, and thus it is easier to implement for materials requiring dopants. Typically, transparent YAG ceramics sintered by this approach have grain sizes over 20 μm.[12,14] Konoshima Chemical Inc. uses co-precipitated YAG powders. Transparent materials synthesized by the co-precipitation approach have grain sizes below 5 μm and mass segregation issues during processing are avoided. One of the limitations of the commercial development of YAG-based laser gain media is that high quality, stoichiometric doped YAG powders are not yet commercially available.

Polycrystalline Nd:YAG has several advantages over Czochralski single crystals including increased dopant homogeneity, lower processing temperatures and times, near net shape forming, increased dopant concentrations, access to more dopants, and possibilities for increased scalability.[12] Also, ceramic processing allows the addition of functional dopant gradients to aid thermal management, increase pump efficiency, and to add other functional elements such as Q-switches to the gain medium.[18]

YAG has a cubic crystal structure with a lattice constant of 12.01 Å and belongs to the space group Ia3d. Y^{3+} (0.1019 nm) is coordinated by 8 O^{2-} ions in the form of a triangular dodecahedron. Two types of Al^{3+} sites exist, one with CN^{IV} (0.039 nm), and a second with CN^{VI} (0.0535 nm).[19] For most laser applications, rare earth elements substitute (Nd^{3+} (0.1109 nm), Er^{3+}

Table 1
Optical and Thermal Properties of Selected Transparent Ceramics

Properties	$Y_3Al_5O_{12}$	$MgAl_2O_4$	Al_2O_3	ALON
Theoretical transmission at 1064 nm (%)*	83.8	86.5	85.4	84.9
Refractive index at 1064 nm	1.82	1.72	1.76	1.78
Transmission range (μm)	0.2–5	0.2–6.5	0.2–6	0.25–6.0
Thermal conductivity (W/m K)	12.9	14.6	24	12.6
Coefficient of thermal exp. (10^{-6}/°C)	7.8	8.0	8.1	7.8
Primary use	Laser Host	Armor	Lighting Envelopes	Armor

The theoretical transmission (%T) is calculated from $T = 100[1 - ((n-1)/(n+1))^2]^2$ where n is the refractive index of the material.

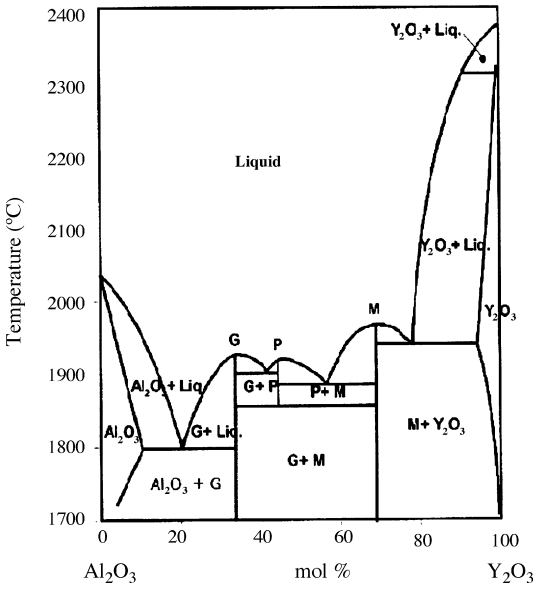

Fig. 1. Y_2O_3–Al_2O_3 phase diagram.[20]

(0.1004 nm), Yb^{3+} (0.0985 nm), etc.) for Y^{3+} in the lattice, and solid solubility of these dopants is affected by the size difference between the dopant and the Y^{3+} ions[19]. The phase diagram for the Y_2O_3–Al_2O_3 system is shown in Fig. 1.[20] YAG ($Y_3Al_5O_{12}$) is a line compound which has important ramifications on processing; any non-stoichiometry in the material appears as second phase scattering sites which may limit optical transmission. Despite the importance of Nd:YAG transparent ceramics, there is virtually no literature pertaining to the importance of SiO_2 and Nd_2O_3 on achieving fully transparent YAG. The objective of this article is to systematically examine the effects of SiO_2 on densification and microstructure development in pure and Nd:YAG.[12,14]

3. Experimental procedure

Al_2O_3 (BA-15, >99.99% pure, specific surface area 16.3 m^2/g, Baikowski Malakoff Inc., Malakoff, TX), Y_2O_3, (BB, >99.99%, specific surface area 35.4 m^2/g, ShinEtsu Co., Tokyo, Japan), Nd_2O_3 (>99.99%, NYC Co., Tokyo, Japan) and tetraethoxysilane (TEOS, 99.9999%, Alfa Aesar, Ward Hill, MA) were used to prepare five YAG compositions: pure YAG, 0.14 wt.% SiO_2 doped YAG, 0.14 wt.% SiO_2 doped 1 at% Nd:YAG, 0.14 wt.% SiO_2 doped 5 at% Nd:YAG, and 0.14 wt.% SiO_2 doped 9 at% Nd:YAG. Since Nd^{3+} substitutes for Y^{3+} in the structure, it is important to compensate for the addition of Nd^{3+} during batching.

Powder batches were ball milled in anhydrous alcohol (reagent grade, 0.04% water, ethanol:methanol 100:5 by volume, J.T. Baker, Phillipsburg, NJ) for 24 h using high purity Al_2O_3 balls (99.9%, 5 mm diameter, Nikkato Corp., Sakai, Japan). The volume ratio of powder:balls:alcohol was 1:4:8. The milled suspensions were dried in an oven, ground in an alumina mortar and passed through a 90 μm screen. The powders were uniaxially pressed into 12.7 mm diameter pellets and cold isostatically pressed at 200 MPa.

Samples were sintered to as high as 1850 °C for up to 16 h in a tungsten mesh heated vacuum furnace (M60, Centorr Vacuum Industries, Nashua, NH) under 5×10^{-6} Torr. The heating and cooling rates were 20 °C/min and 40 °C/min, respectively. Three samples were used for each sintering condition.

Sintered density was measured using the Archimedes method. For SEM analysis (XL20, Philips, Eindhoven, Netherlands), the samples were first polished using a diamond wheel and then sequentially with silk pads with diamond slurries are 6, 3, and 1 μm. The polished specimens were thermally etched at 1400–1550 °C for 30 min. Grain sizes and pore sizes of the sintered samples were obtained by the linear intercept method (200 grains counted).[21] The average grain size and pore size were calculated by multiplying the average linear intercept distance by 1.56. The average pore volume in the samples was calculated, assuming spherical pore shape, by multiplying the average pore volume times the number of pores per unit volume.

For confocal spectroscopic characterization, room temperature fluorescence spectra were recorded by a WITec alpha300 S device using a tunable Argon laser coupled into a single mode optical fiber.[22] The signal was collected in backscattering geometry with a 100× magnification (numerical aperture, N.A. = 0.9 in air) and focused into a multi-mode fiber adjustable with micrometer precision. The core of the multimode fiber (50 μm), acts as the pinhole for confocal microscopy. The end of the fiber is directly connected to the spectrometer and the signal is detected with a Peltier-cooled charge coupled device camera. A beam splitter and notch filter were used to attenuate the pump laser line. Three different gratings with 600, 1200 and 1800 lines/mm blazed at 500 nm were employed depending on the desired spectral resolution. The sample was placed on a 3-axis stage, piezoelectrically controlled in all three directions, thus precise positioning of the sample under the laser spot was achieved (3 nm in the XY direction). For the 514 nm excitation wavelength, the laser was focused to a diffraction-limited spot size of about 355 nm.

4. Densification and grain growth in pure YAG

As noted above, phase formation occurs during sintering in SSR compacts. An earlier study reported that YAG phase formation is complete by 1450 °C for the same materials in this paper.[23] By 1484 °C, SSR compacts are single phase (garnet) and 85% dense. Fig. 2 shows the relative density and grain size for YAG ceramics sintered between 1484 and 1850 °C for 2 h.

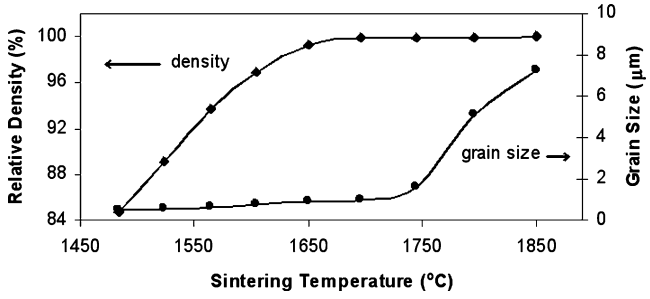

Fig. 2. Densification and grain growth behavior of pure YAG sintered at 1484–1850 °C for 2 h.

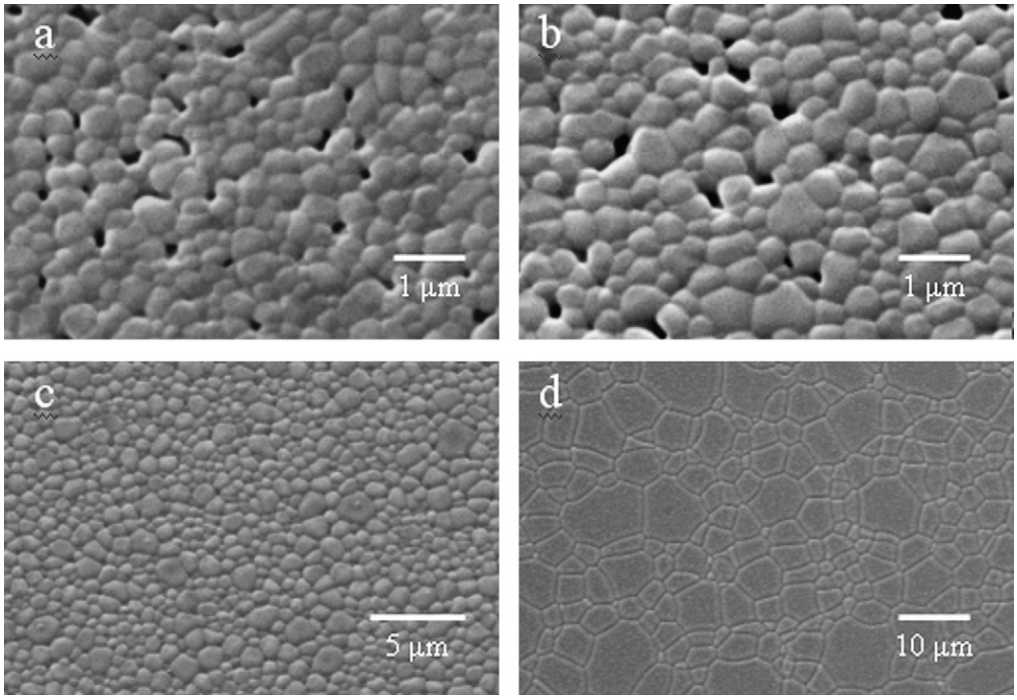

Fig. 3. SEM micrographs of pure YAG sintered for 2 h at (a) 1484 °C, (b) 1564 °C, (c) 1696 °C and (d) 1850 °C.

The density of the samples increases with increasing sintering temperature; closed porosity (92% theoretical density) occurs at about 1550 °C and samples approach 99.9% density by 1696 °C. Surprisingly, there is virtually no grain growth (0.8 μm and 1.2 μm at 1484 and 1696 °C, respectively) in this system even though the sample is near full density. However, samples sintered between 1796 and 1850 °C show a 3–4 time increase in grain size. Fig. 3 shows SEM micrographs of samples sintered between 1484 and 1850 °C for 2 h.

Note that the sample sintered at 1484 °C has pores with varying coordination number (i.e. the number of grains surrounding each pore), but at 1564 °C almost all of the pores have a coordination number ≥ 6 with a diameter similar to the grain size. Kingery and Francois showed the relationship between pore coordination number and its stability as a function of grain size.[24] Based on topological arguments and assuming a dihedral angle near 120°, they showed that pores with a grain coordination number of 6 or greater (in two dimensions) are thermodynamically stable.[24] Fig. 4 shows the average pore radius and number of pores per unit volume for YAG samples sintered between 1484 and 1650 °C for 2 h. The number of pores per unit volume decreases with increasing sintering temperature while the average pore radius increases. Clearly, in YAG there is little grain growth up to 1696 °C (from Fig. 3), thus pore coalescence due to grain growth does not occur. Instead, pores with coordination numbers less than 6 are eliminated because they are thermodynamically unstable. To remove the larger pores, the grain size must increase to satisfy the critical grain size to pore size ratio. The average pore volume is 150,500 vol ppm at 1484 °C but is reduced to 8256 vol ppm by sintering to 1650 °C. Ikesue et al. demonstrated that it is important to lower the pore volume below 150 vol ppm to achieve 84% transmission.[25]

Fig. 5 shows that the activation energies for densification and grain growth (or coarsening) in pure YAG are 235 kJ/mol and 946 kJ/mol, respectively. This is a surprising result because the activation energy for densification is greater than grain growth in most ceramic systems.[26] The fine microstructure observed here is consistent with the analysis performed by Brook, in which he indicated that the grain size versus density trajectory during sintering is controlled by the relative magnitudes of the activation energies for coarsening and densification.[26,27] The uniformity of the microstructures in Fig. 3 may be another reason for the lack of grain growth in the system. This effect is demonstrated in Figs. 2 and 3, where densification is nearly complete by 1650 °C, but little grain growth has occurred.

These results suggest that it may be possible to sinter SSR powders to full density with little to no grain growth, as long as the sample is sintered below the temperature where coarsening becomes thermodynamically favorable over densification (i.e. 1750 °C). However, the requirement for achieving trans-

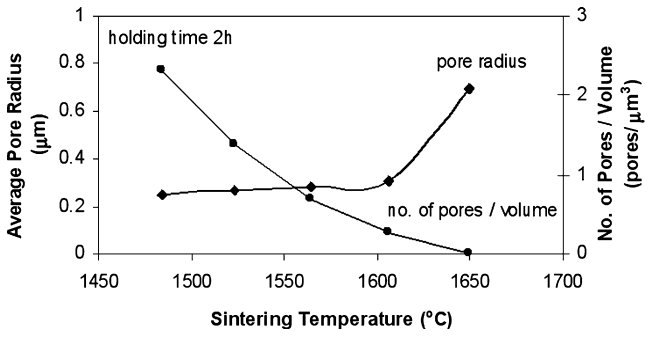

Fig. 4. Average pore radius and number of pores per unit volume for pure YAG sintered at 1484–1650 °C for 2 h.

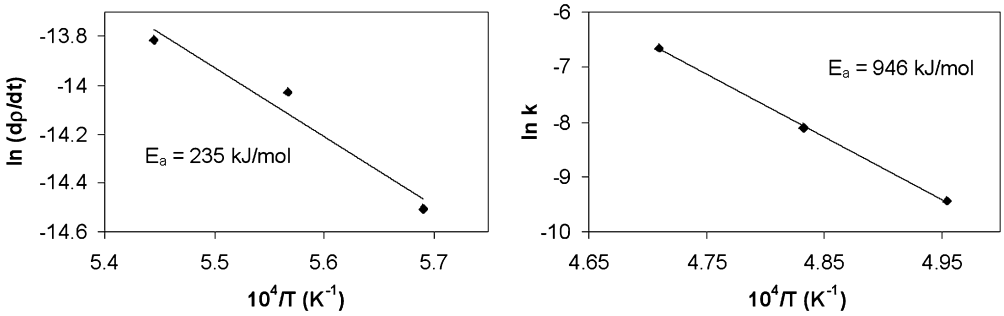

Fig. 5. Activation energy for densification (left) and grain growth (right) in pure YAG.

parency in fine grained ceramics (<5 μm average grain size) is to prevent the occurrence of large pores (i.e. ≥2 μm) that are thermodynamically stable. Since large pores are most likely a result of powder processing and forming, the importance of these processes is clear for ceramics requiring full density.

5. The effect of SiO_2 on densification and grain growth

SiO_2 was added to pure YAG to study its effect on microstructure development and to separate the effect of Nd_2O_3 on sintering of SiO_2 doped Nd:YAG. Fig. 6 shows the relative density versus temperature for both pure and silica doped YAG sintered between 1484 and 1850 °C for 2 h. Densification is significantly enhanced between 1484 and 1750 °C, and the sintering temperature required to achieve full density is reduced by 100 °C in the SiO_2 doped samples. Fig. 7 shows SEM micrographs of samples sintered between 1484 and 1850 °C for 2 h. Note that the samples show no porosity at 1606 °C and the average grain size is still less than 2 μm. However, by 1850 °C, the average grain size has increased to 25 μm. Fig. 8 shows the average grain size versus sintering temperature for both pure and SiO_2 doped samples sintered between 1484 and 1850 °C for 2 h. Between 1484 and 1650 °C the grain size increases from 0.5 to 1.5 μm, but the average grain size increases to 25 μm by 1850 °C in the SiO_2 doped sample. The computed phase diagram of the $Y_3Al_5O_{12}$–SiO_2 system in Fig. 9 shows that a liquid phase begins to form around 1400 °C in SiO_2 doped YAG.[28] This indicates that the enhanced

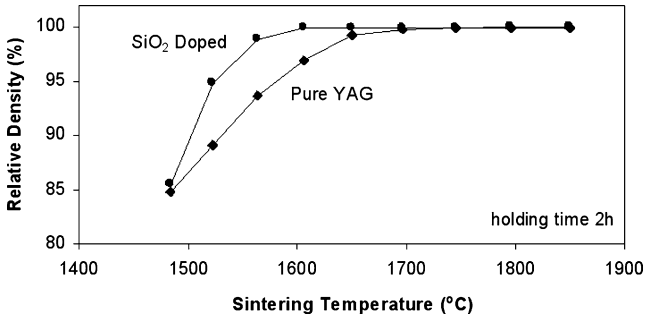

Fig. 6. Relative density vs. temperature for both pure YAG and SiO_2 doped YAG sintered between 1484 and 1850 °C for 2 h.

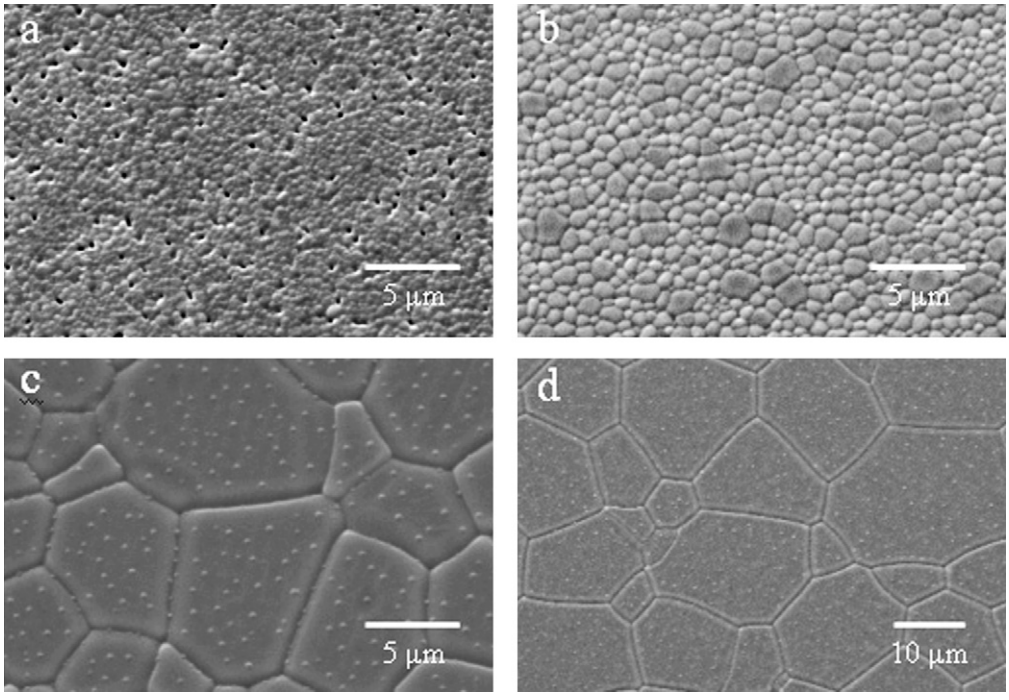

Fig. 7. SEM micrographs of SiO_2 doped YAG sintered for 2 h at (a) 1484 °C, (b) 1606 °C, (c) 1745 °C and (d) 1850 °C.

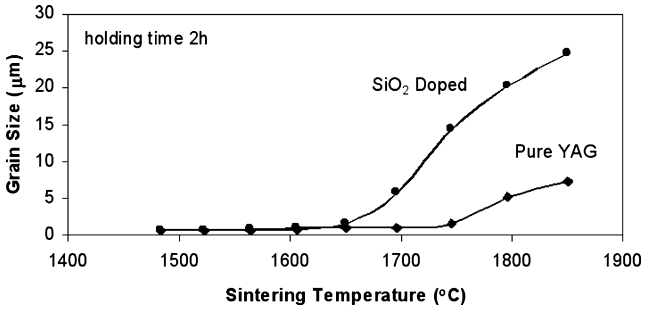

Fig. 8. Grain growth vs. temperature for both pure YAG and SiO_2 doped YAG sintered between 1484 and 1850 °C for 2 h.

densification in the SiO_2 doped YAG is a result of liquid phase sintering. The average grain size increase above 1750 °C in the SiO_2 doped sample relative to the pure YAG sample (over 17 μm at 1850 °C) is also explained by liquid phase enhanced transport.

The grain growth kinetics of both pure and SiO_2 doped YAG sintered at 1745 °C fit the grain growth model:

$$G^n - G_o^n = kt \quad (1)$$

where G is the average grain size, G_o is the initial grain size, k is a rate constant, and t is time. The pure YAG samples fit an $n=2$ dependence and the SiO_2 doped samples fit an $n=3$ dependence. As described by Brook, a grain growth exponent of 2 indicates that solid state mass transport is the dominant mechanism for coarsening while $n=3$ indicates that liquid phase mass transport occurs in the sample (for the case of boundary controlled migration).[29]

6. Optically active ions and densification and grain growth in YAG

Fig. 10 shows the effect of Nd^{3+} on density for SiO_2 doped YAG sintered between 1484 and 1850 °C for 2 h. Samples doped

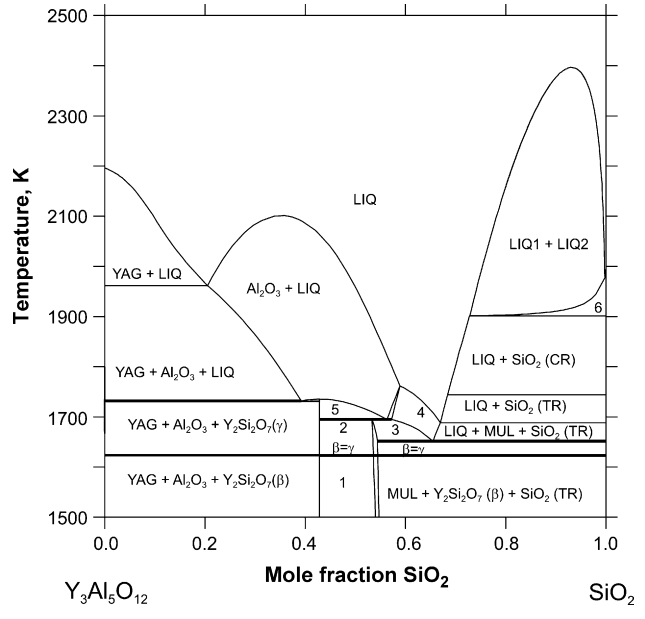

Fig. 9. YAG–SiO_2 phase diagram.[28]

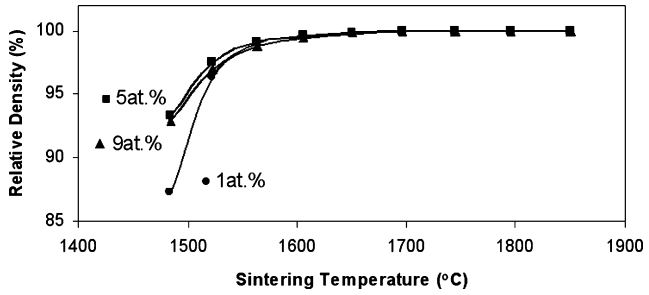

Fig. 10. Relative density vs. temperature for 0.14 wt.% SiO_2 doped 1, 5, and 9 at% Nd:YAG sintered for 2 h.

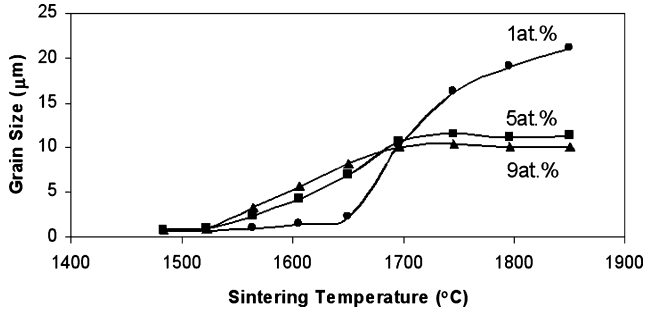

Fig. 11. Grain size vs. temperature for 0.14 wt.% SiO_2 doped 1, 5, and 9 at% Nd:YAG sintered between 1484 and 1850 °C for 2 h.

with higher concentrations of Nd^{3+} showed higher sintered densities (87% for 1 at% Nd^{3+} vs. 93% for 9 at% Nd^{3+}) between 1484 and 1600 °C. Fig. 11 shows that samples with a greater Nd^{3+} content underwent enhanced grain growth between 1523 and 1700 °C (2 μm and 8 μm average grain size at 1650 °C for 1 and 9 at% Nd^{3+}, respectively). As shown in the Nd_2O_3-SiO_2 binary phase diagram (Fig. 12), Nd_2O_3 forms a liquid phase with SiO_2, and while the exact composition of the liquid phase is unknown in the quaternary Y_2O_3–Al_2O_3–Nd_2O_3–SiO_2, Nd_2O_3 may increase the amount of liquid phase present leading to enhanced liquid phase sintering and increased densification and grain growth rates.[30]

Fig. 11 also shows that grain growth at temperatures above 1650 °C scales inversely with Nd^{3+} concentration (e.g. 21 and 10 μm for 1 and 9 at% Nd^{3+} at 1850 °C, respectively). The plot

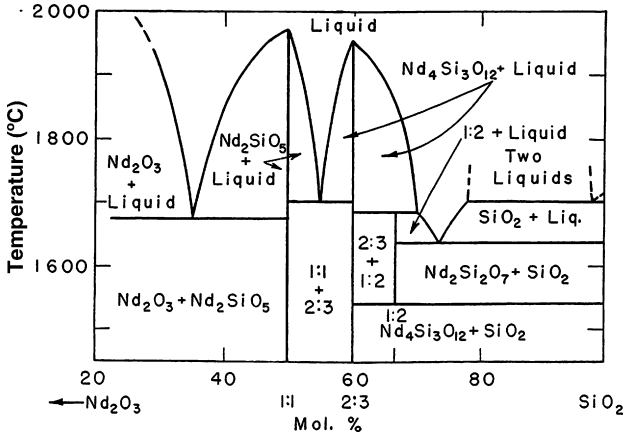

Fig. 12. SiO_2–Nd_2O_3 phase diagram.[30]

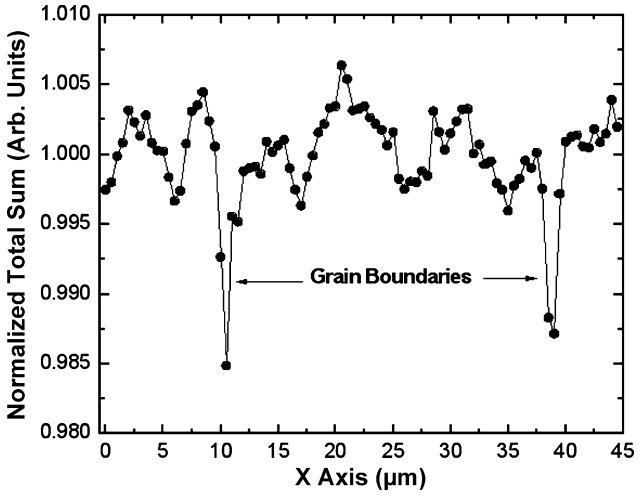

Fig. 13. Detail of the total emission area corresponding to crossing two grain boundaries using fluorescence confocal scanning optical microscopy. Nd^{3+} and SiO_2 concentration were 1 at% and 0.14 wt.% respectively. The sample was sintered at 1850 °C for 16 h.

in Fig. 13 is a line scan of a confocal fluorescence scanning optical microscopy image where the intensity is inversely proportional to the Nd^{3+}.[31] The intensity profile shows that the Nd^{3+} content at grain boundaries is higher than the bulk. To interpret this figure it is important to note that intensity decreases at the grain boundaries because higher Nd^{3+} content quenches the fluorescence signal used to probe Nd^{3+} location. The high temperature grain growth behavior shown in Fig. 11, combined with the increased Nd^{3+} content at grain boundaries shown in Fig. 13, may be explained by solute drag effects as first explored by Cahn.[32] Presumably, Nd^{3+} has a lower diffusion constant than either Y^{3+} or Al^{3+} due to its increased atomic mass and ionic radius; therefore, as the grains grow Nd^{3+} may begin to collect at grain boundaries effectively slowing coarsening in the sample. It should be noted that decreased grain growth above 1700 °C in higher Nd^{3+} content samples may also be explained by the slower diffusion of Nd^{3+} in the bulk separate from solute drag effects.

7. Summary

Densification and grain growth in YAG, SiO_2 doped YAG, and SiO_2 doped Nd:YAG ceramics were explored with special emphasis on the effects of SiO_2 and Nd_2O_3. Pure YAG sinters by solid state diffusion and near full density is reached by 1700 °C. The activation energy for coarsening is higher than densification in pure YAG indicating that samples can be sintered to near full density with little to no grain growth provided that no thermodynamically stable pores are present in the sample. SiO_2 doped YAG densifies by liquid phase sintering. SiO_2 doped YAG sinters to full density at 100 °C lower than pure YAG and also shows significantly increased coarsening at higher temperatures. SiO_2 doped Nd:YAG shows enhanced sintering and grain growth at low temperatures relative to SiO_2 doped YAG, most likely due to increased liquid phase content. At temperatures above 1700 °C, high Nd^{3+} content Nd:YAG has a smaller grain size than low Nd^{3+} content Nd:YAG, possibly due to solute drag effects.

Acknowledgement

This work was supported by VLOC Inc. through funds received from VLOC's prime contract #N66001-00-c-6008. S.K. is particularly grateful for the support of a Royal Thai Scholarship. We also thank E. Meuschke and Baikowski Malakoff Inc. for supplying the BA-15 alumina powder used in this study. The authors also wish to thank A. Ikesue for helpful conversations.

References

1. Coble, R. L., Transparent alumina and method of preparation. US Patent 3026210, 20 March, 1962.
2. Anderson, R. D., Transparent yttria-based ceramics and method for producing same. US Patent 3545987, 8 December, 1970.
3. Benecke, M. W., Olsen, N. E. and Pask, J. A., Effect of LiF on hot-pressing of MgO. *J. Am. Ceram. Soc.*, 1967, **50**, 365–368.
4. Roy, D. W. and Stermole, F. J., Method for manufacturing a transparent ceramic body. US Patent 3974249, 10 August, 1976.
5. McCauley, J. W. and Corbin, N. D., Phase relations and reaction sintering of transparent cubic aluminumoxynitride spinel (ALON). *J. Am. Ceram. Soc.*, 1979, **62**, 476–479.
6. Gentilman, R. L., MaGuire, E. A., and Dolhert, L. E., Transparent aluminum oxynitride and method of manufacture. US Patent 4520116, 28 May, 1985.
7. Gentilman, R. L., Fusion-casting of transparent spinel. *Am. Ceram. Soc. Bull.*, 1981, **60**, 906–909.
8. Apetz, R. and van Bruggen, M. P. B., Transparent alumina: a light-scattering model. *J. Am. Ceram. Soc.*, 2003, **86**, 480–486.
9. Krell, A., Blank, P., Ma, H., van Bruggen, M. P. B. and Apetz, R., Transparent sintered corundum with high hardness and strength. *J. Am. Ceram. Soc.*, 2003, **86**, 12–18.
10. Greskovich, C. and Chernoch, J. P., Polycrystalline ceramic lasers. *J. Appl. Phys.*, 1973, **44**, 4599–4606.
11. de With, G. and van Dijk, H. J. A., Translucent $Y_3Al_5O_{12}$ ceramics. *Mater. Res. Bull.*, 1984, **19**, 1669–1674.
12. Ikesue, A., Kinoshita, T., Kamata, K. and Yoshida, K., Fabrication and optical properties of high performance polycrystalline Nd:YAG ceramics for solid state lasers. *J. Am. Ceram. Soc.*, 1995, **78**, 1033–1040.
13. Lu, J., Prabhu, M., Song, J., Li, C., Xu, J., Ueda, K. *et al.*, Optical properties and highly efficient laser oscillation of Nd:YAG ceramics. *J. Appl. Phys. B*, 2000, **71**, 469–473.
14. Lee, S.-H., Kochawattana, S., Messing, G. L., Dumm, J. Q., Quarles, G. and Castillo, V., Solid-state reactive sintering of transparent polycrystalline Nd:YAG ceramics. *J. Am. Ceram. Soc.*, 2006, **89**, 1945–1950.
15. Lu, J., Takaichi, K., Uematsu, T., Shirakawa, A., Musha, M., Ueda, K. *et al.*, Promising ceramic laser material: highly transparent Nd^{3+}:Lu_2O_3 ceramic. *Appl. Phys. Lett.*, 2002, **81**, 4324–4326.
16. Lu, J., Takaichi, K., Uematsu, T., Shirakawa, A., Musha, M., Ueda, K. *et al.*, Yb^{3+}:Y_2O_3 ceramics—A novel solid-state laser material. *Jpn. J. Appl. Phys. Part 2: Lett.*, 2002, **41**, L1373–L1375.
17. Lupei, V., Lupei, A. and Ikesue, A., Transparent Nd and (Nd, Yb)-doped Sc_2O_3 ceramics as potential new laser materials. *Appl. Phys. Lett.*, 2005, **86**, 111118.
18. Ikesue, A., Aung, Y. L., Kamimura, T., Yoshida, K., and Messing, G. L., "Progress in Ceramic Lasers", in Annual Reviews in Materials, eds. V. Gopalan, G. Wegner, D. R. Clarke, M. Ruhle and J. Bravman, 2006, **36**, pp. 397–429.
19. Shannon, R. D. and Prewitt, C. T., Effective ionic radii in oxides and fluorides. *Acta Crystallogr. Sect. B*, 1969, **25**, 925–946.
20. Mizuno, M. and Noguchi, T., *Rept. Govt. Ind. Res. Inst. Nagoya*, 1967, **16**, 171.

21. Fullman, R. L., Measurement of Particle Sizes in Opaque Bodies. *Trans. AIME*, 1953, **197**, 447–452.
22. Lee, S.-H., Stitt, J., White, W.B., Messing, G.L., Gopalan, V., "Spatial mapping of fluorescence and Raman spectra across grain boundaries in a transparent Nd-YAG ceramic laser material", Proceedings of SPIE - The International Society for Optical Engineering, Volume 6100 – Solid State Lasers XV: Technology and Devices H. J. Hoffman, R. K. Shori, Eds, (Feb 28, 2006) 6100, art. no. 610011.
23. Kochawattana, S., Lee, S.-H., Misture, S., and Messing, G. L., Size effects on yttrium aluminum garnet (YAG) phase formation. J. Am. Ceram. Soc., in review.
24. Kingery, W. D. and Francois, B., Sintering of crystalline oxides, 1. Interactions between grain boundaries and pores. In *Sintering and Related Phenomena*, ed. G. C. Kuczynski, N. A. Hooton and G. F. Gibbon. Gordon Breach, New York, 1967, pp. 471–498.
25. Ikesue, A. and Yoshida, K., Influence of pore volume on laser performance of Nd:YAG ceramics. *J. Mater. Sci.*, 1999, **34**, 1189–1195.
26. Brook, R. J., Production of ceramics with superior mechanical properties. *Proc. Brit. Ceram. Soc.*, 1982, **32**, 7–24.
27. Harmer, M. P., Roberts, E. W. and Brook, R. J., Rapid sintering of pure and doped alpha-Al_2O_3. *Trans. J. Br. Ceram. Soc.*, 1979, **78**, 22–25.
28. Fabrichnaya, O., Seifert, H. J., Weiland, R., Ludwig, T., Aldinger, F. and Navrotsky, A., Phase equilibria and thermodynamics in the Y_2O_3-Al_2O_3-SiO_2 system. *Z. Metallkd.*, 2001, **92**, 1083–1097.
29. Brook, R. J., Controlled grain growth. In *Ceramic Fabrication Processes, Treatise on Materials Science and Technology*, *9*, ed. F. F. Y. Wang. Academic Press, New York, 1976, p. 331.
30. Miller, O. and Rase, D. E., Phase Equilibrium in the System Nd_2O_3-SiO_2. *J. Am. Ceram. Soc.*, 1964, **47**, 653–654.
31. Ramirez, M. O., Wisdom, J., Li, H., Aung, Y. L., Stitt, J., Messing, G. L., Dierolf, V., Liu, Z., Ikesue, A., Byer, R. L., and Gopalan, V., 3-dimensional grain boundary spectroscopy in transparent high power ceramic laser materials, Opt. Exp., in review.
32. Cahn, J. W., The impurity drag effect in grain boundary motion. *Acta Met.*, 1962, **10**, 789–798.